Taylor & Francis
Taylor & Francis Group

High Pressure Research
An International Journal

ISSN: (Print) (Online) Journal homepage: https://www.tandfonline.com/loi/ghpr20

Pressure calibration based on the ultrasonic measurement in multi-anvil apparatus

Wei Song, Qizhe Tang, Chang Su, Xiang Chen & Yonggang Liu

To cite this article: Wei Song, Qizhe Tang, Chang Su, Xiang Chen & Yonggang Liu (2021) Pressure calibration based on the ultrasonic measurement in multi-anvil apparatus, High Pressure Research, 41:1, 75-87, DOI: 10.1080/08957959.2020.1863398

To link to this article: https://doi.org/10.1080/08957959.2020.1863398

HIGH PRESSURE RESEARCH
2021, VOL. 41, NO. 1, 75–87
https://doi.org/10.1080/08957959.2020.1863398

Taylor & Francis
Taylor & Francis Group

Pressure calibration based on the ultrasonic measurement in multi-anvil apparatus

Wei Song [a], Qizhe Tang[a,b], Chang Su[c], Xiang Chen[a,b] and Yonggang Liu[a]

[a]Key Laboratory of High-Temperature and High Pressure Study of the Earth's Interior, Institute of Geochemistry, Chinese Academy of Sciences, Guiyang, People's Republic of China; [b]University of Chinese Academy of Sciences, Beijing, People's Republic of China; [c]Institute of Disaster Prevention, Sanhe, People's Republic of China

ABSTRACT

Two ultrasonic measurement methods for pressure calibration to 4.4 GPa in a multi-anvil apparatus by measuring the travel times of longitudinal wave as a function of pressure are reported. The first method is to continuously calibrate pressure by combining the measured travel times of Z-cut quartz under hydrostatic pressure with the related equation of state and unit-cell parameters of quartz. The second method is fixed-point calibration, which is to calibrate the pressure by measuring the abrupt change of the longitudinal wave travel times since the samples, H_2O, Hg and Bi used in this study will undergo pressure-induced phase transitions at room temperature. Experimental results of these two methods are in good agreement. The quartz pressure scale obtained from this study is expressed as $P(\mathrm{GPa}) = 28.7(1-t_p/t_{p0})$. The two ultrasonic measurement methods might be complementary means for pressure calibration in situations where other probe method is not conveniently available.

ARTICLE HISTORY
Received 2 September 2020
Accepted 3 December 2020

KEYWORDS
Pressure calibration; ultrasonic measurement; phase transition; multi-anvil apparatus

Introduction

The precise determination of pressure has been a long-standing and essential problem for high pressure experimentation. In general, methods for the determination of pressure in various types of high pressure devices include (1) fixed-point calibration, which is based on phase transitions of metals and semiconductors (*e.g.* Bi, Ba, ZnTe, ZnS, and GaAs), and (2) continuous pressure calibration, which is to build relationships between pressure and certain experimentally measurable properties of a given material, such as changes in resistance (*e.g.* manganin), unit-cell volume (*e.g.* NaCl, Au, and MgO), peak shifts in fluorescence (Ruby) and Raman spectra (diamond, c-BN).

In principle, travel times/sound velocities of well-characterized materials also can be used as pressure markers. Previously, single crystal olivine [1] and polycrystalline alumina ceramics buffer rod [2] have been used as *in-situ* pressure markers in ultrasonic measurements in multi-anvil apparatus (MAA). At present, with regard to optimal

CONTACT Yonggang Liu Liuyonggang@mail.gyig.ac.cn Key Laboratory of High-Temperature and High Pressure Study of the Earth's Interior, Institute of Geochemistry, Chinese Academy of Sciences, Guiyang 550081, People's Republic of China

ultrasonic method for pressure measurement in MAA, it has to be combined with synchrotron X-ray diffraction, and X-ray radiography technique, allowing for simultaneous measurements of longitudinal wave and shear wave travel times, specific volume (density), and sample length on specimens, then an absolute pressure scale can be derived [3,4]. However, few high pressure experiments can fulfill these stringent requirements of scientific instrument. To this end, recently Wang et al. [5] developed a new method for *in-situ* pressure determination in MAA in conjunction with synchrotron X-radiation using an acoustic travel times approach, which was obtained by calibrating the travel times of the polycrystalline alumina ceramics buffer rod against the NaCl scale. Although the new *in-situ* alumina ceramics pressure gauge is expected to be utilized for offline laboratory studies, it's a reliable pressure scale only when offline experiments can be provided with the same sample assembly (especially the same alumina ceramics buffer rod) and stress conditions.

Another ultrasonic method for pressure determination is the phase transition determination, which is analyzing the travel times (sound velocities) between two distinct phases, especially the liquid–solid phase transitions, which will typically exhibit the striking travel times (velocities) contrast. According to the abrupt change of travel times of the sample across the different phase boundaries of bismuth, Wang et al. [6] calibrated the relation of sample pressure and oil pressure of MAA. But no effective cross validation exists in their experiments. Officer and Secco [7] proposed a technique for detecting and measuring phase transitions in MAA by measuring the travel times of longitudinal wave that travel through a pressure cell containing a Hg sample as a function of pressure. However, this technique is few used probably for being more complex to implement and yielding ambiguous results.

In this study, we measured the travel times of three kinds of samples, Hg, H_2O and Bi at room temperature in a MAA, when which undergo phase transitions, that are liquid Hg to α Hg, α Hg to β Hg, liquid H_2O to ice VI, and Bi I to Bi II, respectively. Based on the results of the travel times as a function of oil pressure, the sample pressure is calibrated by combining the corresponding pressure of phase transition known in literature. Moreover, as a cross validation, we also presented a new Z-cut quartz pressure scale, which is used to continuously calibrate the pressure by combining the measured travel times of quartz under hydrostatic pressure with the related equation of state and unit-cell parameters of quartz from literature.

Experiment methods

The experiments are performed on a MAA (DS3600t), which is capable of generating oil pressures up to 90 MPa (about 4 GPa, the diameter of the ram piston is 230 mm), at the Key Laboratory for High- Temperature and High Pressure Study of the Earth's Interior, Institute of Geochemistry, Chinese Academy of Sciences, China.

Two similar sample assemblies, A and B, were used in this study, and schematic diagram of the sample assemblies are shown in Figure 1(a) and (b), respectively. Assembly A is used in ultrasonic measurements of Hg and H_2O and assembly B is used in ultrasonic measurements of Bi and Z-cut quartz. In assembly A, a cylindrical tungsten carbide (WC, 6 mm in diameter, 4.75 mm in length) holder with a groove (3 mm in width, 1.25 mm in depth in Hg experiment and 1.50 mm in depth in H_2O experiment) was used as an

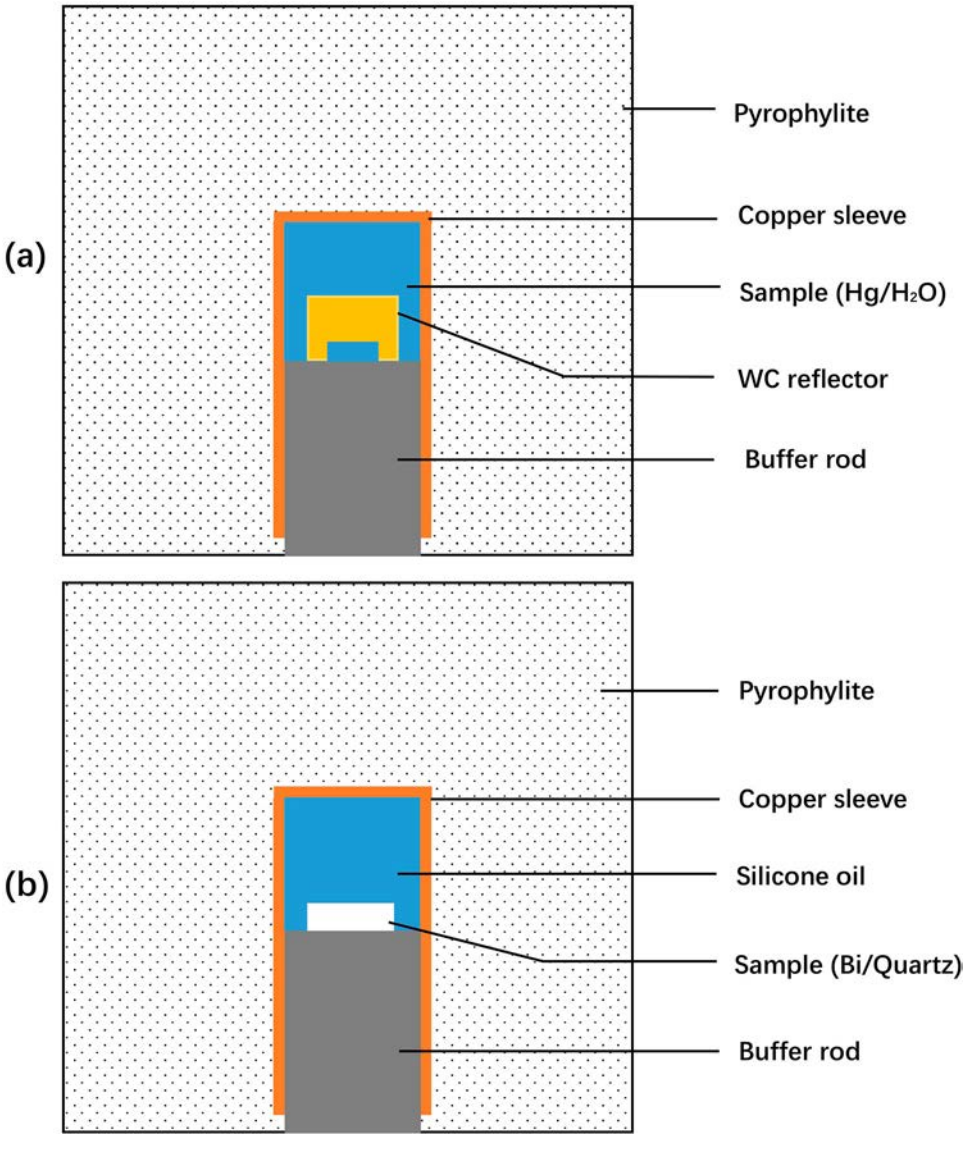

Figure 1. Schematic diagram of the sample assemblies used in this study. (a) and (b) represent assembly A and assembly B, respectively.

acoustic reflector so as to limit the sample length under the high pressure [8–10]. WC is affixed to the polycrystalline alumina ceramics buffer rod (8 mm in diameter, 12 mm in length) by inorganic glue at the side. The surrounding of WC is filled with deionized water or mercury (analytical reagent), and a copper sleeve is used to prevent the sample from leaking. No distortion was observed in the WC and groove after the experiments, and the depth of the groove remained the same. Aided by the equation of state of WC, the dimensional changes of the WC reflector under pressures to 5 GPa were estimated to be very slight and negligible [8–10]. In another word, within the

pressure scope of this study, the length of the sample under high pressure can be assumed to be constant. In assembly B, sample Bi (99.99% purity, 5 mm in diameter, 1.68 mm in length) or sample Z-cut quartz single crystal ($\rho_0 = 2.65$ g/cm^3, 5 mm in diameter, 1.81 mm in length) is affixed to the polycrystalline alumina ceramics buffer rod by inorganic glue at the side. The surrounding of sample is filled with silicon oil to provide hydrostatic pressure environment. All contact interfaces include the buffer rod, WC and solid sample are well polished before the measurements and this is critical to ensure no material, neither surrounding liquid nor glue, will be squeezed into the contact interfaces between the buffer rod and WC/solid sample under pressure [9].

The ultrasonic travel times are measured with the classical pulse-echo method by using a longitudinal wave ultrasonic transducer with 10 MHz center frequency, a digital oscilloscope (Tektronix DPO2024B, U.S.A.) and an ultrasonic pulse generator/receiver unit (CTS-8077PR, Guangdong Goworld Co., Ltd., Shantou, China). Detailed descriptions of the ultrasonic measurement system have been given by Liu et al. [11]. A part of the received ultrasonic wave signals is shown in Figure 2. Signals in Figure 2(a) are from Hg experiment using assembly A, and signals in Figure 2(b) are from *Z*-cut quartz experiment using assembly B. In Figure 2(a), the black and red waveform correspond to echoes before and after the solidification induced by increasing the oil pressure, respectively. Echo 1 and Echo 2 represent the longitudinal wave signal reflected from the buffer rod–sample and the sample–silicon oil/(WC) interface, respectively. After liquid–solid phase transition, the echo 2 signal rapidly moved forward and as it can be seen in Figure 2(a), the travel time in the sample decreased obviously. The travel times in the sample was determined by the interval between the two corresponding peaks shown in Figure 2(a,b). The travel time measurement sensitivity is 0.4 ns, and the relative uncertainty is less than 0.1%. The depth error of the WC groove is about 9 μm (include zero pressure and high pressure conditions), and the corresponding relative uncertainty of travel time is about 0.6%. Considering the system error, we believe that the whole uncertainty of travel time is about 1% for assembly A and 0.5% for assembly B, respectively.

Results and discussion

All experimental results of travel times in the samples as a function of oil pressure are shown in Table 1 and we will make use of it to pressure calibration in this section successively.

Travel times in H_2O

The phase diagram of H_2O by Choukroun and Grasset [12] and the loading path of this study are shown in Figure 3. With the oil pressure increasing, the travel times in H_2O are decreasing as shown in Figure 4. It is obvious that at oil pressure ~13.5 (±0.5) MPa, the travel times in H_2O decrease sharply, which suggests that H_2O transforms into ice VI phase at this oil pressure. The melting curves of ice VI (the transition pressure of H_2O to ice VI) have been studied frequently, and Choukroun and Grasset [12] summarized

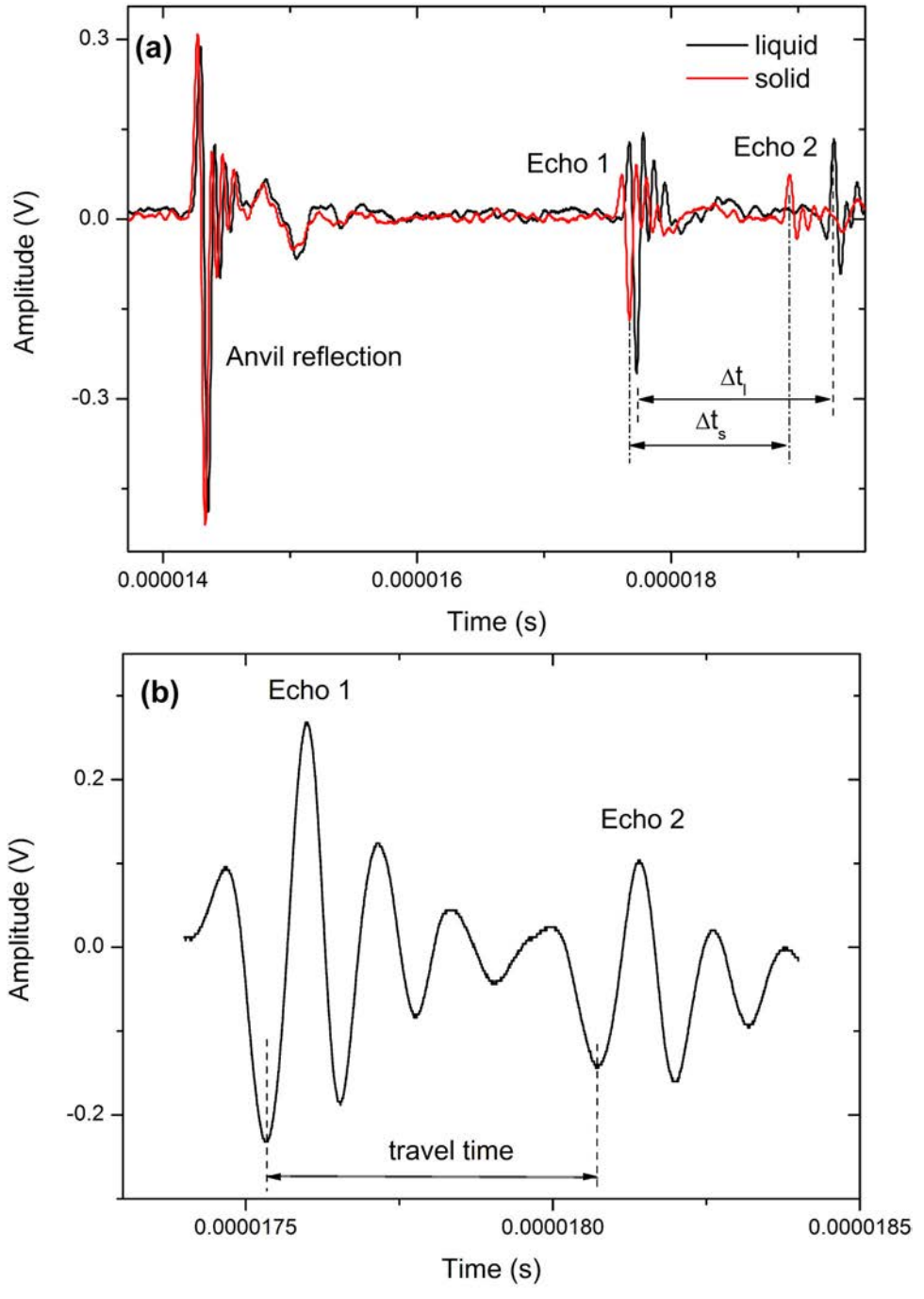

Figure 2. Acoustic signals observed under high pressure. (a) is observed before and after liquid Hg-α Hg phase transition in Hg experiment using assembly A, and (b) is observed at 20 MPa oil pressure in quartz experiment using assembly B. Echo 1: buffer, Echo 2: sample. Δt_l: travel time in liquid sample, Δt_s: travel time in solid sample.

Table 1. The change of travel times in H_2O, Hg, Bi and Z-cut quartz with increasing of oil pressure.

P_{oil} (MPa)	t_p-H_2O (μs)	P_{oil} (MPa)	t_p-Hg (μs)	P_{oil} (MPa)	t_p-Bi (μs)	P_{oil} (MPa)	P (GPa)	t_p-SiO_2 (μs)
6	1.4700	10	1.6022	15	1.5066	0	0	0.5691*
7	1.3920	12	1.5808	20	1.4870	6	0.28	0.5658
8	1.3178	15	1.5480	25	1.4342	8	0.45	0.5618
9	1.3100	16	1.5402	30	1.4018	10	0.53	0.5598
10	1.2518	17	1.5336	33	1.3820	15	0.86	0.5520
11	1.2472	18	1.5300	35	1.3766	20	1.44	0.5390
12	1.2012	18.85	1.2832	36	1.3654	30	2.11	0.5254
13	1.1622	20	1.2142	37	1.3576	35	2.46	0.5186
14	0.7204	22	1.2038	38	1.3560	40	2.61	0.5158
15.2	0.6544	25	1.1812	39	1.3532	45	2.95	0.5096
16	0.6348	30	1.1622	40	1.3640	50	3.05	0.5078
17	0.6228	38.4	1.1376	41	1.3588	55	3.33	0.5028
18	0.6188	42	1.1308	42	1.3452	60	3.57	0.4986
19	0.6180	46	1.1146	43	1.3482	70	3.89	0.4932
20	0.6142	50	1.1050	44	1.3390	80	4.08	0.4900
22	0.6086	53	1.0992	46	1.3264	90	4.42	0.4844
24	0.6068	56.4	1.0936					
26	0.6026	58	1.0688					
28	0.5912	58.8	0.9678					
30	0.5880	60	0.8620					
		64	0.8562					
		67	0.8532					
		70	0.8504					

Note: The travel time in *Z*-cut quartz at zero pressure is from linear fitting the travel times under high pressure.

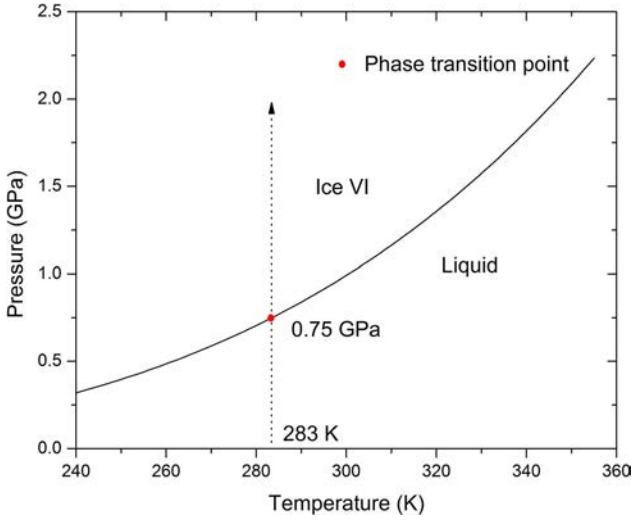

Figure 3. Phase diagram of H_2O by Choukroun and Grasset and loading path of this study.

the experimental data in those studies to present a Simon-Glatzel equation referring the relation between the melting pressure and temperature:

$$P_m(\text{GPa}) = 0.6184 + 0.6614 \times ((\frac{T_m(K)}{272.73})^{4.69} - 1) \quad (1)$$

where P_m and T_m denote the melting pressure and temperature. Thereby it's readily to

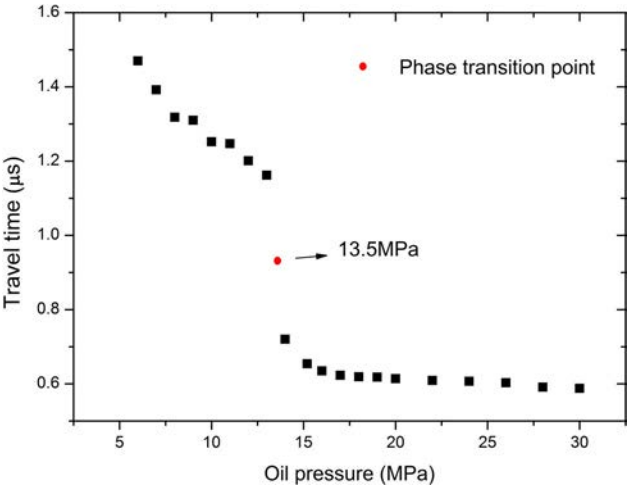

Figure 4. Travel times in H_2O under high pressure.

calibrate the sample pressure by the using of travel times in H_2O and the specific experimental temperature.

Travel times in Hg

The phase diagram of Hg by Cannon [13] and loading path of this study are shown in Figure 5. With the oil pressure increasing up to 70 MPa, the travel times in Hg are shown in Figure 6. At oil pressure ~18.4 (±0.4) MPa and ~58.5(±0.3) MPa, the travel times decrease dramatically, resulted from the phase transitions, liquid Hg to α Hg and α Hg to β Hg, respectively.

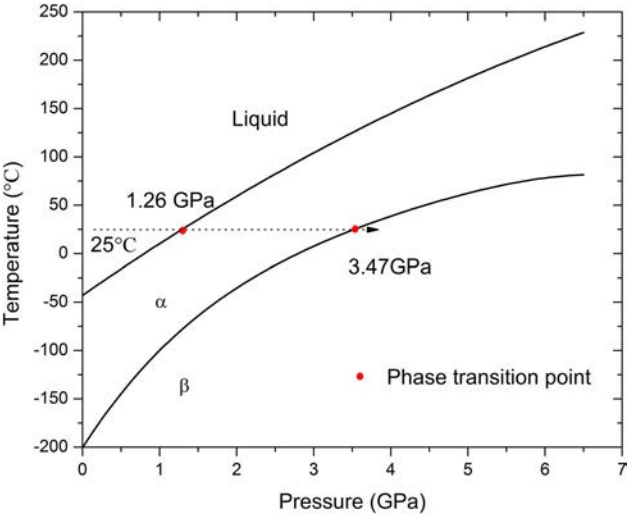

Figure 5. Phase diagram of Hg by Cannon and loading path of this study.

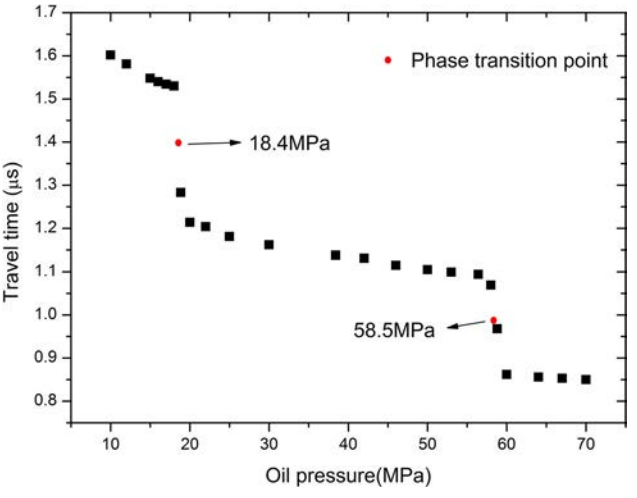

Figure 6. Travel times in Hg under high pressure.

The transition pressure of mercury at 0°C, which has been successfully determined at 0.76 GPa [14], is one of the well-known fixed-points for pressure calibration. Moreover, it's suggested that investigations on the melting pressures for many other temperatures, that is the mercury melting curve, could be used as a practical pressure scale. Molina et al. [15] determined the mercury melting curve up to 1.2 GPa with high accuracy and he fitted all of his 52 experimental points with a third-order polynomial, resulting in the following equation:

$$P(MPa) = 19.32835d + 0.0017068d^2 + 0.000060867d^3 \quad (2)$$

where $d = \mathrm{T(K)}-234.309$.

With regard to the transition pressure of α Hg to β Hg, there are some direct experimental data available from Bridgman [16], which are used to polynomial fitting to obtain the following relation:

$$P(\mathrm{GPa}) = 0.00006t^2(^\circ\mathrm{C}) + 0.0233t(^\circ\mathrm{C}) + 2.8464 \quad (3)$$

Based on the travel times in Hg and Equations (2) and (3), the sample pressures at the two oil pressure points have been determined.

Travel times in Bi

Bismuth is of great interest metal at high pressure and is being widely used as a pressure calibrator in the past decades. At room temperature, the Bi I–II transition pressure was observed at 2.52 GPa [17]. The travel times in Bi sample under high pressure in this study are shown in Figure 7. At oil pressure ~39.5 (±0.5) MPa, the travel times increase abnormally, so we believed the I–II transition take place at this oil pressure. This trend was also observed in Wang's study [6], in which they further determined the Bi II–III transition by using travel times of longitudinal and shear wave. We only measured the longitudinal wave travel time of sample Bi, which is difficult to be used to determine the II–III

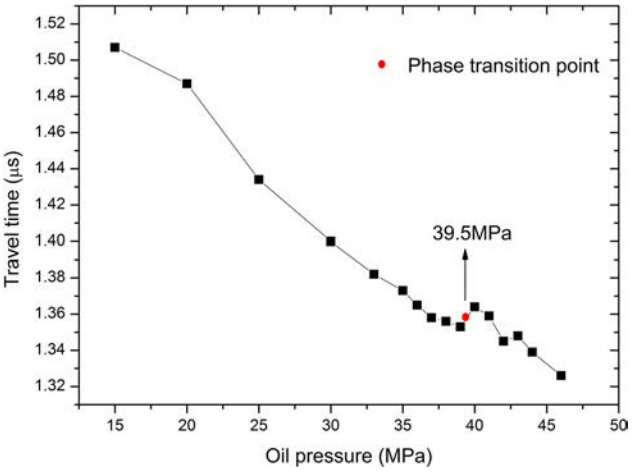

Figure 7. Travel times in Bi under high pressure.

phase transition. Therefore, we did not use Bi II–III phase transition to calibrate the pressure in this study.

Z-cut quartz pressure calibration

Quartz is one of the most common minerals in the Earth's crust and can be used as an internal pressure standard for high pressure experiments in diamond-anvil cell [18,19]. In this section, we will make use of the travel times in *Z*-cut quartz under hydrostatic pressure at room temperature to calibrate the sample pressure.

For *Z*-cut quartz, we can get the following formula:

$$v_{33} = \sqrt{\frac{c_{33}}{\rho}} \tag{4}$$

$$c_{33} = c_{33}^0 + c_{33}' P \tag{5}$$

$$t = \frac{2l}{v_{33}} \tag{6}$$

$$\frac{\rho}{\rho_0} = \frac{V_0}{V} \tag{7}$$

where v_{33} is sound velocity in Z direction, ρ is density, V is volume, subscript '0' represents values at zero pressure, c_{33} is the elastic modulus in Z direction, $c_{33}^0$and $c_{33}'$are elastic modulus at zero pressure and its pressure derivative, both are available from McSkimin et al. [20] ($c_{33}^0 = 105.75\,\text{GPa}$, $c_{33}' = 10.84$), P is pressure, t is the travel times in quartz, l is the length of quartz under high pressure, which can be obtained by polynomial fitting data of Angel *et al*. [18] on the unit-cell parameters of quartz:

$$\frac{l}{l_0} = 1 - 0.00729P + 0.00068P^2 - 0.000005P^3 + 0.00000014537P^4 \tag{8}$$

and the relation between V/V_0 and l/l_0 also can be obtained:

$$\frac{V}{V_0} = -20.013 + 38.544(\frac{l}{l_0}) - 17.531(\frac{l}{l_0})^2 \tag{9}$$

Using Equations (4)–(7), we will find:

$$t = \frac{2l}{\sqrt{\frac{c_{33}^0 + c'_{33}P}{\rho_0(\frac{V}{V_0})^{-1}}}} \tag{10}$$

As l_0, ρ_0, c_{33}^0, c'_{33} are known, combining Equations (8)–(10), Equation (10) is in fact referring the relation between t and P, every P value yields a corresponding t value. Therefore, we can calculate a set of travel times t by changing pressure P value, and when the calculated travel time matches precisely (accurate to 0.1 ns) the measured travel time at a specific oil pressure in ultrasonic experiment, we can get the relation between the sample pressure and the oil pressure, then the sample pressure can be calibrated.

The travel times in quartz under high pressure in this study are shown in Figure 8. Using the method presented above, the sample pressure is determined as shown in Figure 9. After polynomial fitting, the pressure calibration curve is expressed as$P(\text{GPa}) = -0.2605 + 0.0893P_{oil}(\text{MPa}) - 0.0004P_{oil}^2(\text{MPa})$, where P_{oil} is oil pressure.

Figure 10 shows the normalized travel times of quartz as a function of pressure. After linear fitting, the quartz pressure scale is expressed as $P(\text{GPa}) = 28.7(1\text{-}t_p/t_{p0})$. Note that, this quartz pressure scale is appropriate for pressure determination below 4.4 GPa and the pressure determined using this scale is estimated to have a standard error <0.1 GPa. For higher pressure determination, it still needs more validation tests.

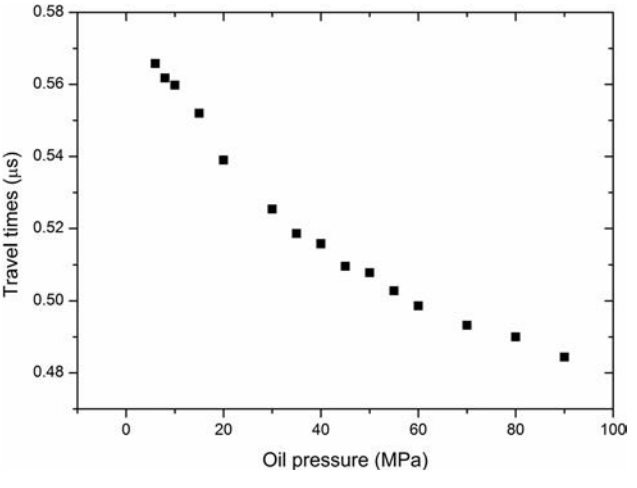

Figure 8. Travel times in quartz under high pressure.

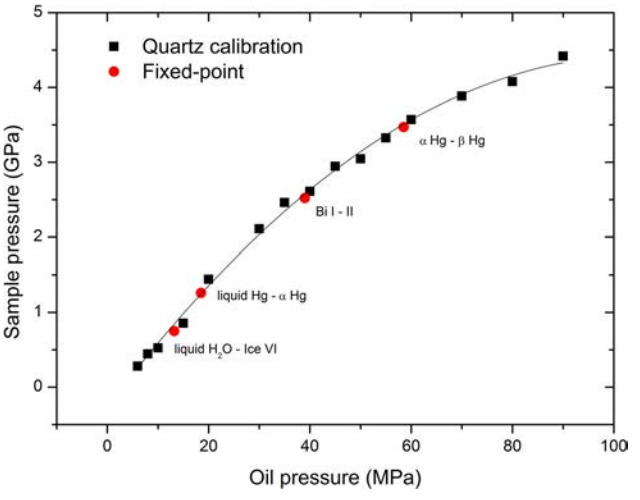

Figure 9. Comparison of pressure determined using Z-cut quartz as pressure marker with calibration from fixed-point method. Error bars are within the symbol size.

Cross validation

The results of the two ultrasonic methods for pressure calibration are showed in Figure 9. As compared in Figure 9, the four discrete pressure points derived from the fixed-point method exactly locate in the continuous pressure calibration curve derived from the new Z-cut quartz pressure calibration method, yielding excellent mutual agreement. Therefore, it's proved that the ultrasonic measurement methods employed in this study are valid for pressure calibration in MAA.

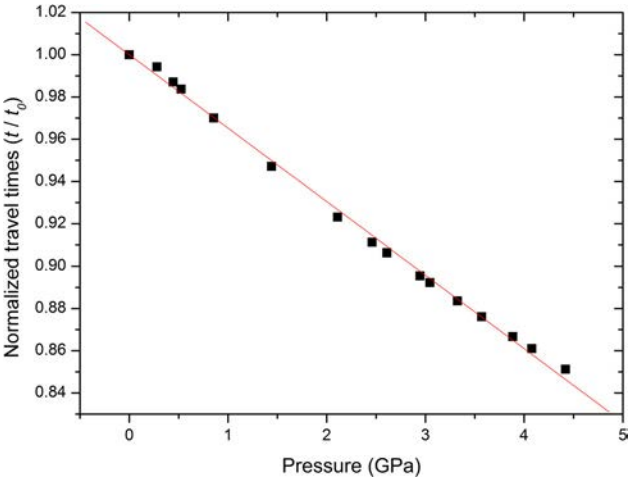

Figure 10. Normalized travel times of quartz as a function of pressure. The red line is the linear fitting result to normalized travel times.

Conclusion

Two ultrasonic measurement methods for pressure calibration to about 4.4 GPa in multi-anvil apparatus by measuring the travel times of longitudinal wave as a function of oil pressure are reported. The results of the two ultrasonic measurement methods for pressure calibration are in excellent agreements with each other, and so the validities of the two ultrasonic methods for pressure calibration are confirmed. Meanwhile, the accuracies of the corresponding phase transition pressure of H_2O, Hg and Bi used in this study also verified the consistency of these various pressure calibration systems. These ultrasonic methods might be complementary means for pressure calibration in situations where other probe method cannot be conveniently available. Moreover, it's worth noting that the Z-cut quartz also can be used as a good internal pressure marker candidate for *in-situ* pressure determination.

Acknowledgements

This work was supported by the National Natural Science Foundation of China under grant number 41873075 and the West Light Foundation of The Chinese Academy of Sciences. We thank Dr Wenge Zhou at the Institute of Geochemistry in the Chinese Academy of Sciences for helpful discussion.

Disclosure statement

No potential conflict of interest was reported by the author(s).

Funding

This work was supported by the National Natural Science Foundation of China under [grant number 41873075] and the West Light Foundation of The Chinese Academy of Sciences.

ORCID

Wei Song http://orcid.org/0000-0001-9640-6766

References

[1] Sinelnikov Y, Chen G, Liebermann RC. Dual mode ultrasonic interferometry in multi-anvil high pressure apparatus using single-crystal olivine as the pressure standard. High Pressure Res. 2004;24:183–191.
[2] Higo Y, Inoue T, Li B, et al. The effect of iron on the elastic properties of ringwoodite at high pressure. Phys Earth Planet. Inter. 2006;159:276–285.
[3] Li B, Kung J, Uchida T, et al. Pressure calibration to 20 GPa by simultaneous use of ultrasonic and X-ray techniques. J Appl Phys. 2005;98(1):013521.
[4] Li B, Liebermann RC. Study of the Earth's interior using measurements of sound velocities in minerals by ultrasonic interferometry. Phys Earth Planet Inter. 2014;233:135–153.
[5] Wang X, Chen T, Qi X, et al. Acoustic travel time gauges for in-situ determination of pressure and temperature in multi-anvil apparatus. J Appl Phys. 2015;118:065901.
[6] Wang Z, Liu Y, Bi Y, et al. Hydrostatic pressure and temperature calibration based on phase diagram of bismuth. High Pressure Res. 2012;32(2):167–175.
[7] Officer T, Secco RA. Detection of a P-induced liquid ⇌ solid-phase transformation using multiple acoustic transducers in a multi-anvil apparatus. High Pressure Res. 2015;35(3):289–299.

[8] Song W, Liu Y, Wang Z, et al. Note: measurement method for sound velocity of melts in large volume press and its application to liquid sodium up to 2.0 GPa. Rev Sci Instrum. 2011;82:086108.
[9] Wang Z, Liu Y, Zhou W, et al. Sound velocity in water and ice up to 4.2 GPa and 500 K on multi-anvil apparatus. Chin Phys Lett. 2013;30(5):054302.
[10] He Z, Wang Z, Zhu H, et al. High-pressure behavior of amorphous selenium from ultrasonic measurements and Raman spectroscopy. Appl Phys Lett. 2014;105:011901.
[11] Liu Y, Xie H, Zhou W, et al. A method for experimental determination of compressional velocities in rocks and minerals at high pressure and high temperature. J Phys: Condens Matter. 2002;14:11381.
[12] Choukroun M, Grasset O. Thermodynamic model for water and high-pressure ices up to 2.2 GPa and down to the metastable domain. J Chem Phys. 2007;127:124506.
[13] Cannon JF. Behavior of the elements at high pressures. J Phys Chem Ref Data. 1974;3(3):781–824.
[14] Ruoff AL, Lincoln RC, Chen YC. A new method of absolute high pressure determination. J Phys D: Appl Phys. 1973;6:1295.
[15] Molinar GF, Bean V, Houck J, et al. The mercury melting line up to 1200 MPa. Metrologia. 1980;16:21–29.
[16] Bridgman PW. Polymorphism, principally of the elements, up to 50, 000 kg/cm^2. Phys Rev. 1935;48:893–906.
[17] Getting IC. New determination of the Bi I-II equilibrium pressure: a proposed modification to the practical pressure scale. Metrologia. 1998;35:119–132.
[18] Angel RJ, Allan DR, Miletich R, et al. The use of quartz as an internal pressure standard in high-pressure crystallography. J Appl Cryst. 1997;30:461–466.
[19] Chervin JC, Ch P, Polian A. Quartz as a pressure sensor in the infrared. High Pressure Res. 2005;25(2):97–105.
[20] McSKimin HJ, Andreatch P JR, Thurston RN. Elastic moduli of quartz versus hydrostatic pressure at 25° and −195.8°C. J Appl Phys. 1965;36(5):1624–1632.